PAPER • OPEN ACCESS

Design and analysis of automobile components using industrial procedures

To cite this article: B Kedar *et al* 2017 *IOP Conf. Ser.: Mater. Sci. Eng.* **263** 062035

View the article online for updates and enhancements.

Design and analysis of automobile components using industrial procedures

B Kedar, B Ashok, Nisha Rastogi and Siddhanth Shetty
School of Mechanical Engineering, VIT University, Vellore - 632014, Tamil Nadu, India.

Email id: ashok.b@vit.ac.in

Abstract: Today's automobiles depend upon mechanical systems that are crucial for aiding in the movement and safety features of the vehicle. Various safety systems such as Antilock Braking System (ABS) and passenger restraint systems have been developed to ensure that in the event of a collision be it head on or any other type, the safety of the passenger is ensured. On the other side, manufacturers also want their customers to have a good experience while driving and thus aim to improve the handling and the drivability of the vehicle. Electronics systems such as Cruise Control and active suspension systems are designed to ensure passenger comfort. Finally, to ensure optimum and safe driving the various components of a vehicle must be manufactured using the latest state of the art processes and must be tested and inspected with utmost care so that any defective component can be prevented from being sent out right at the beginning of the supply chain. Therefore, processes which can improve the lifetime of their respective components are in high demand and much research and development is done on these processes. With a solid base research conducted, these processes can be used in a much more versatile manner for different components, made up of different materials and under different input conditions. This will help increase the profitability of the process and also upgrade its value to the industry.

1. Introduction
An integral component of today's automobiles is the steering system and its associated linkages which are essential in assisting the driver to maintain the direction and stability of the vehicle. The different type of steering systems includes worm and nut gears, recirculating ball gears, worm and sector gears and rack and pinion gears. The Design analysis for the automobile components namely, the rack gear has been carried out in this report for analyzing the material using a new design. The process to be simulated is Induction Hardening (IH). Induction hardening is a form of heat treatment in which a metal part is heated by induction heating (Here 650-850 °C) and then quenched. The quenched metal undergoes a martensitic transformation, increasing the hardness and brittleness of the part. Induction hardening is used to selectively harden areas of a part or assembly without affecting the properties of the part as a whole. The standard material used is EN8C.

   Rudnev [1] discussed that not all gears and pinions are well suited for induction hardening. Also, it is not always possible to obtain a fully-martensitic hardened case. Depending upon the kind of steel, the presence of some retained austenite within the hardened case is unavoidable. The complications of computer simulation were discussed by Ruffini [2] who concluded that Induction heating process is a

typically complex and diverse process whose features cannot be simulated using a single software program. Induction hardening can be done using various number of coils and in various frequencies such as single coil single frequency, single coil double frequency and double coil double frequency as explained by Rudnev [3]. Magnabosco [4] measured the efficiency of the process and concluded that despite the high heating rate at the surface of the specimen, the very high temperatures reached (about 1250 $^\circ$C) in this zone are able to completely transform the external layer in austenite. Some other advantages of this process were discussed by Coupard [5] who states that "One of the main features of induction surface treatment is the high fatigue strength improvement. It is also viewed as a cleaner process than carburizing because it uses less toxic products than those used in carburizing or nitriding". In their paper Breen [6] concluded that a large hardening depth generate less compressive residual stresses in the hardened layer than a thin one. Their evolution under cyclic loading depends on the local plastic strains experienced during fatigue. Depending on both the residual stress field and the applied external fatigue loading, cracks can either initiate near the surface or beneath the hardened layer. The usage of Finite Element Analysis has been justified by Yuan [7] where it is stated that due to the temperature-dependent nonlinear properties in induction heating process, analytical solutions are difficult to obtain. But, finite element methods (FEM) appear to be superior to others such as finite difference methods. Furthermore, general-purpose commercial finite element programs have been widely used in industry and are becoming more popular for engineering analysis and equipment design. Rapidly heating and quenching the material can induce stresses on its surface, as explained by Pacheco [8] where it is explained that the internal stresses generated during quenching can produce warping and even cracking of a steel body and, therefore, the prediction of such stresses is an important task. Xu [9] concluded that, "An over thick quenching layer with high compressive stress will lead to high tensile residual stress in the tough core, which will reduce the loading capacity and lead to a reduction in the ductility of the component". K. Palaniradja [10] has inferred that optimal control chamber temperature and quench water temperature are two main factors to be considered while the rack and pinion gears undergo surface hardness change and are the optimal factors on which the case depth is decided.

The aim of this project is to compare and contrast, between the theoretical/actual process and analytical/simulative process; on how the various physical and chemical properties of the rack change as it undergoes the process of Induction hardening and see if these properties vary upon the use of different metals as replacements and under a variety of input conditions. The economic constraints on whether the standard material used is cost effective or if a substitute material can be used or not have been discussed along with the results. An experimental simulation has been conducted to observe and differentiate between the electrical input parameters and the thermal output parameters and to note the variations, both graphically and numerically for all of the substitute materials.

Some of the gaps identified at the beginning of simulation were that the initialization of current density distribution on each coil grid is a cumbersome but important step for desired temperature pattern control. Generally, the current density should be stronger in the part of the coil area neighboring concave in work piece. The arrangement of current density distribution for a specially desired heating pattern and hardening pattern may guide real conduction coil design. It was also identified that the current research conducted could not, provide sufficient evidence on what happens if the material subjected to induction hardening process undergoes a change in its chemical structure or if it develops cracks on its outer surface, how would its properties change.

Table 1. IH Operating process

Operation	Process Specification

Scanning Feed	500-520 mm/min
Quenching Feed	600-620 mm/min
Heating Time	15-30 sec
High Quench Conc.	3-5%
Quench Water Temp.	25-35 °C
Quench Water Flow	20-25 LPM
Power	60-65 KW
Quench Time	30-50 sec
Air Pressure	4-6 bar

Table 2. Material Properties

Property	EN8C	Cast Iron	Structural Steel
Cost ($/ton)	500	1200	600
Density (gm/cc)	7.85	7.2	7.8
Tensile Strength(MPa)	>380	200	400-550
Melting Pt. (°C)	1426-1538	1150-1200	1130
Resistivity (ohm m)	1.43 e-7	9.6e-8	1.7e-7
Conductivity	30BTU/ft^2hr(F/ft)	30.045	34.95
Specific Heat	502.42 J/kgK	447	434

Table 3. Material Compositions

Element	EN8C	Cast Iron	Structural Steel
Carbon %	0.17-0.24	0.2-0.4	0.15-0.25
Silicon %	0.17-0.37	0.1-0.3	<0.40
Manganese %	0.7-1.00	0.50	0.75-1.00
Sulphur %	<0.035	<0.02	<0.030
Phosphorus %	<0.035	0.01	<0.040
Chromium %	<0.25	0.20	0.115-0.130
Nickel %	<0.25	0.45	<0.10
Copper %	<0.25	0.01	<0.01

Table 4. Standard Specifications of Surface Hardness and Case Depth

Control Item	Specification
Case Depth Teeth Side	1.27-2.54 mm
Case Depth Back of Bar	0.89-4.32 mm
Hardness Teeth Surface	78-82 HRA
Hardness Back of Bar	73-82 HRA

Induction Hardening Length	200-210 mm

The motivation for this project was obtained to determine the difference in the surface hardness and the case depth for the different materials after the finish of this process and to find out whether any other material could be used as an alternative substitute to increase the profit margins of production. As shown in Table 2 above, the alternative materials chosen were cast iron and structural steel and their chemical composition is mentioned in Table 3 above. Table 1 mentions the standard operating procedure for the IH process.

2. Design and Simulation
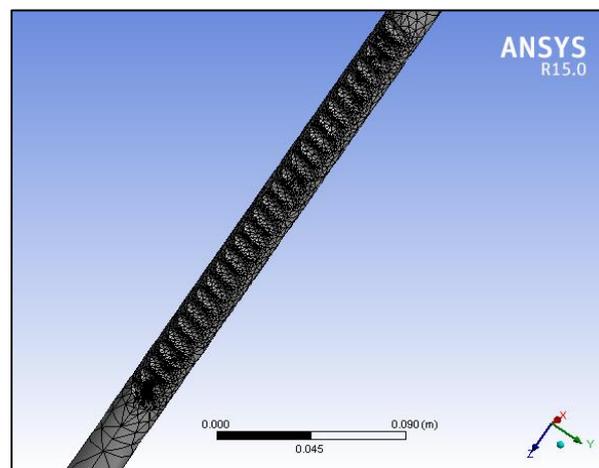
Figure 1. ANSYS (Meshing)

The boundary conditions followed in the present work is mentioned below and these points are considered in the design and analysis of the proposed work.
(i) The model was meshed using tetrahedron method.

(ii) The element was meshed with coarse type and medium smoothing.

(iii) Number of nodes = 3986

(iv) Number of Elements = 2003

(v) After this, the teeth section of the rack was refined further to provide a more accurate simulation model and to give more accurate results.

(vi) Number of nodes (after refinement) = 16380

(vii) Number of elements (after refinement) = 8266

To set-up the thermal-electric simulation, the number of time steps over which the calculation is done is take as 10 (not the default 1) time steps with 1 second per step and an update interval of 2.5 seconds kept as default. This is done so as to provide ample number of iterations and at the same time, to provide a

congruence point in a relatively quicker time [10-12]. Also, the radiosity controls that measure the relation between the radiation convergence and the surface parameters has been kept on with a convergence value of 0.0001 W/m2. Smooth contours have been set to provide details about the variations in the input and output results. The meshed model of the designed structure is shown Figure 1.

The solver used here was of gauss-seidel iterative type. These are the FEM equations needed and used by the solver while analyzing the data given and these are the main equations used for determining the results. The resources for this data were taken from the help section in the project window main screen.

- Biot-Savart Law for finding the magnetic vector potential
- Gauss Law for determining flux density
- Faraday's law for calculating the electric field intensity.
- Ampere's Law for current density (not compulsory).
- Equation for determining Joule Heat Generated.

Taking into account, the real-time conditions present, an input voltage of 525 volts was applied in increasing steps throughout each of the ten time steps with phase voltage set to zero. To improve the accuracy of the readings, the voltage was applied across the 28 teeth only, but the output was generalized throughout the entire surface of the rack. Also as part of the thermal input, the room temperature was maintained at 30 °C and the gear was initially placed at the room temperature. As the voltage was applied, the rack was simultaneously cooled by the surrounding air and the coolant. For this, the convection factor was considered between the outer surface and water. Also, the heat flow was assumed to flow through the rack body and between the rack and the surrounding medium and so the total heat flux was evaluated as part of the results.

3. Results and Discussion
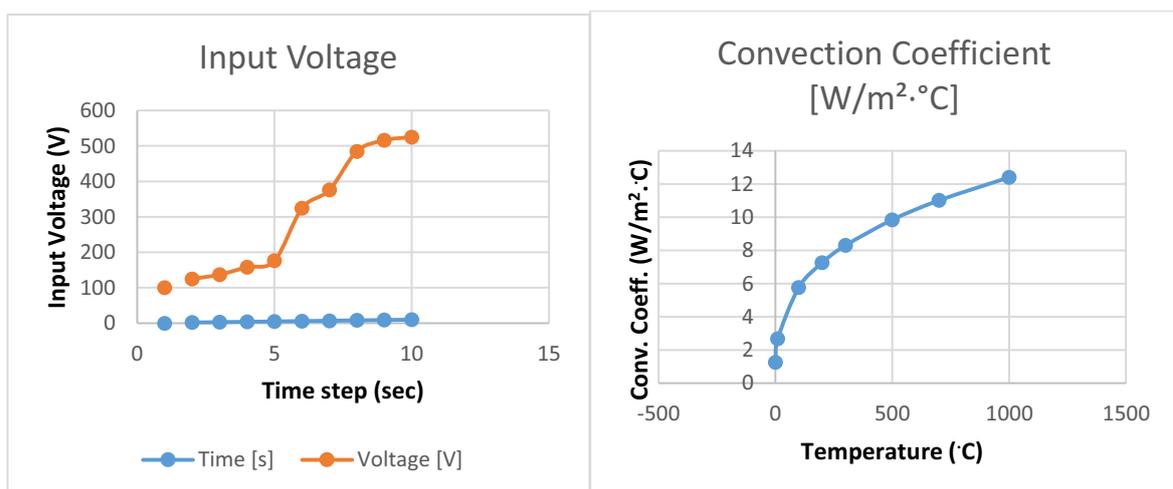
Figure 2(a). Input voltage for IH process

Figure 2(b). Conv. Coefficient for quench water

In the figure 2(a) given above the step increase of the input voltage provided to heat the rack is given in a graphical format to a maximum value of 525 V. Figure 2(b) shows the variation of the Convection Coefficient of quench water with respect to the temperature.

Table 5. (a) Solver Output for Structural Steel

	Electric Voltage	**Joule Heat**	**Total Electric Field Intensity**
	Minimum Value Over Time		
Minimum	100. V	2.1447e-015 W/m³	1.2235e-011 V/m
Maximum	525. V	9.6177e-014 W/m³	9.4967e-011 V/m
	Maximum Value Over Time		
Minimum	100. V	0.31819 W/m³	1.7167e-004 V/m
Maximum	525. V	8.7698 W/m³	9.0127e-004 V/m

Table 5. (b) Temperature for structural steel

	Temperature	**Total Heat Flux**
	Minimum Value Over Time	
Minimum	248.73 °C	10.062 W/m²
Maximum	589.26 °C	1249.6 W/m²
	Maximum Value Over Time	
Minimum	390.55 °C	4.598e+005 W/m²
Maximum	609.44 °C	9.3765e+005 W/m²

Table 6. (a) Solver output for cast iron

	Electric Voltage	**Joule Heat**	**Total Electric Field Intensity**
	Minimum Value Over Time		
Minimum	100. V	8.0742e-015 W/m³	1.0846e-011 V/m
Maximum	525. V	2.3646e-013 W/m³	7.8596e-011 V/m
	Maximum Value Over Time		
Minimum	100. V	0.56343 W/m³	1.7167e-004 V/m
Maximum	525. V	15.531 W/m³	9.013e-004 V/m

Table 6. (b) Temperature for cast iron

	Temperature	Total Heat Flux
Minimum Value Over Time		
Minimum	233.99 °C	9.4547 W/m²
Maximum	588.25 °C	1263.9 W/m²
Maximum Value Over Time		
Minimum	384.57 °C	4.4221e+005 W/m²
Maximum	611.1 °C	9.2758e+005 W/m²

Table 7. (a) Solver output for EN8C

	Electric Voltage	Joule Heat	Total Electric Field Intensity
Minimum Value Over Time			
Minimum	100. V	4.4055e-015 W/m³	1.0291e-011 V/m
Maximum	525. V	1.1376e-013 W/m³	8.415e-011 V/m
Maximum Value Over Time			
Minimum	100. V	0.37828 W/m³	1.7168e-004 V/m
Maximum	525. V	10.426 W/m³	9.013e-004 V/m

Table 7. (b) Temperature for EN8C

	Temperature	Total Heat Flux
Minimum Value Over Time		
Minimum	265.38 °C	8.2511 W/m²
Maximum	589.72 °C	1266.3 W/m²
Maximum Value Over Time		
Minimum	421.04 °C	4.9745e+005 W/m²

Maximum	611.41 °C	9.3048e+005 W/m²

The tables given above 5 to 7, denotes the maximum and minimum value of the output parameters for all of the materials based on the iterations conducted for all the time steps. These values are taken as comparison against the standard values of EN8C. As It is noticeable, for the given input voltage the Joule heat value is the maximum for Cast Iron > EN8C > Structural Steel. This means that maximum heat is produced in Cast Iron for the same voltage. However, the electric field intensity is the maximum for Structural Steel > EN8C > Cast Iron. For Heat Flux Structural Steel > EN8C > Cast Iron. This implies that the rate of heat energy transfer is maximum in Structural Steel and minimum in Cast Iron.
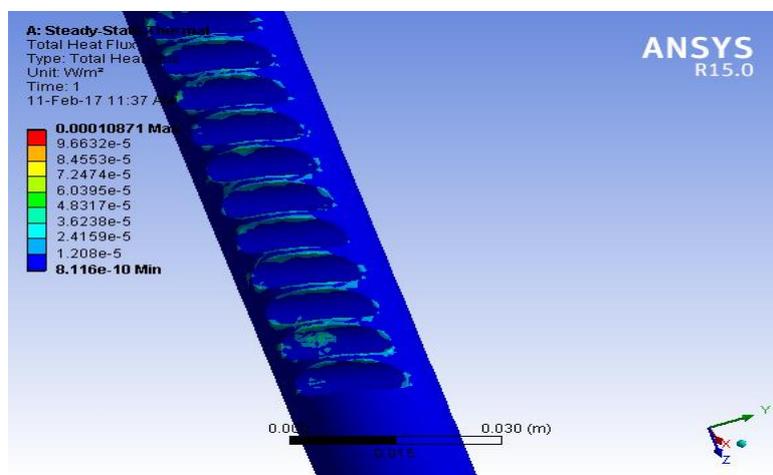
Figure 3(a). Heat flux analysis of Cast Iron Rack Rod
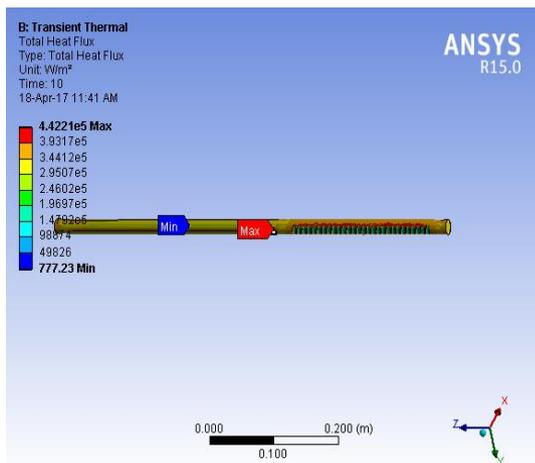
Figure 3(b). Heat flux for cast iron
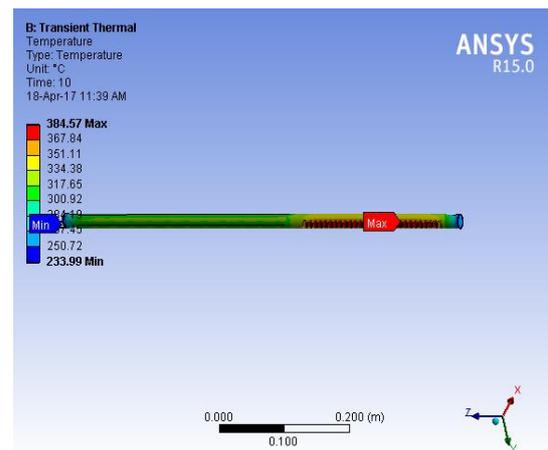
Figure 3(c). Temperature for cast iron
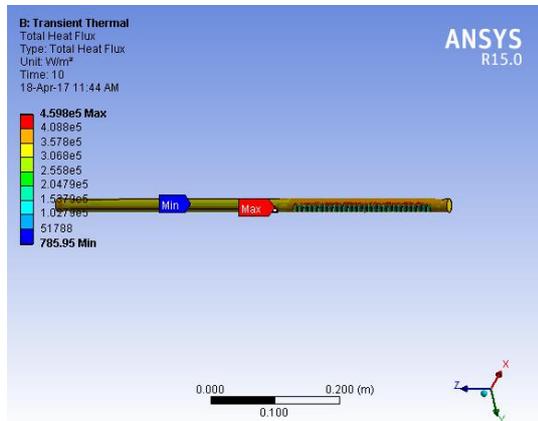
Figure 4(a). Heat flux contours for
structural steel
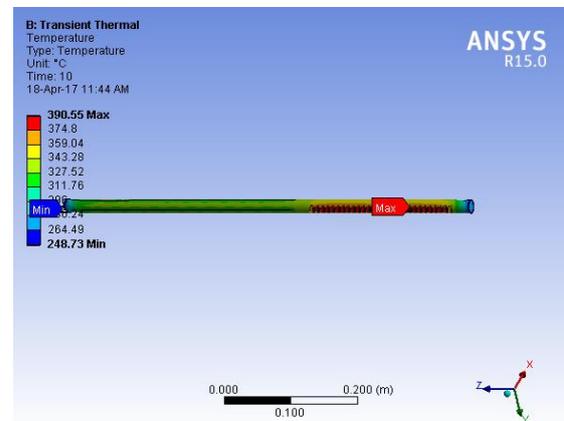
Figure 4(b). Temperature contours for
structural steel
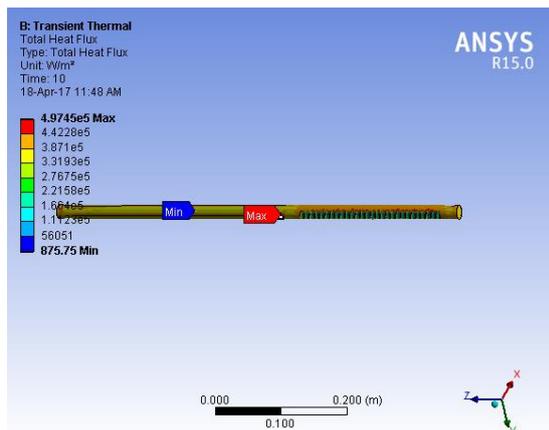
Figure 5(a). Heat flux contours for EN8C
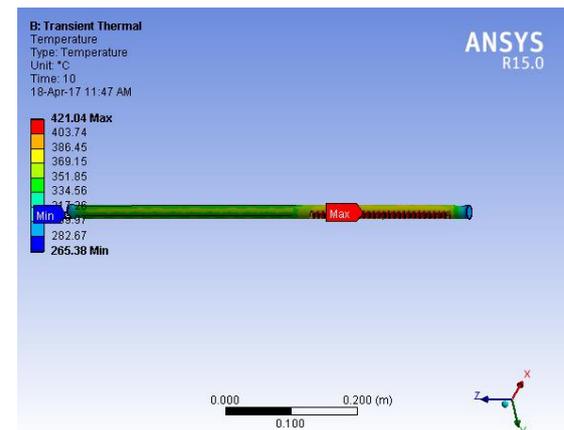
Figure 5(b). Temperature contours for EN8C

Figure 3(a) shown above, is a close up view of the heat flux variation in the teeth section in the rack. As seen, it is not even around the teeth gaps and varies individually. The figures given above depict the contours obtained for the parameters Heat Flux and Temperature for all of the simulated materials. These are based on the iterative values whose boundary limits are mentioned in the tables 5-7. As seen from figures 3(b), 4(a), 5(a) we notice that the Heat Flux is maximum in the teeth region of the rack gear and starts decreasing as we move across the length of the rod. This is due to the dispersion by conduction and convection to the quench water. The same can be derived for the Temperature contours in 3(c), 4(b), 5(b). Here the temperature drop is noticeable right from the edge of the teeth section throughout the length of the rack.
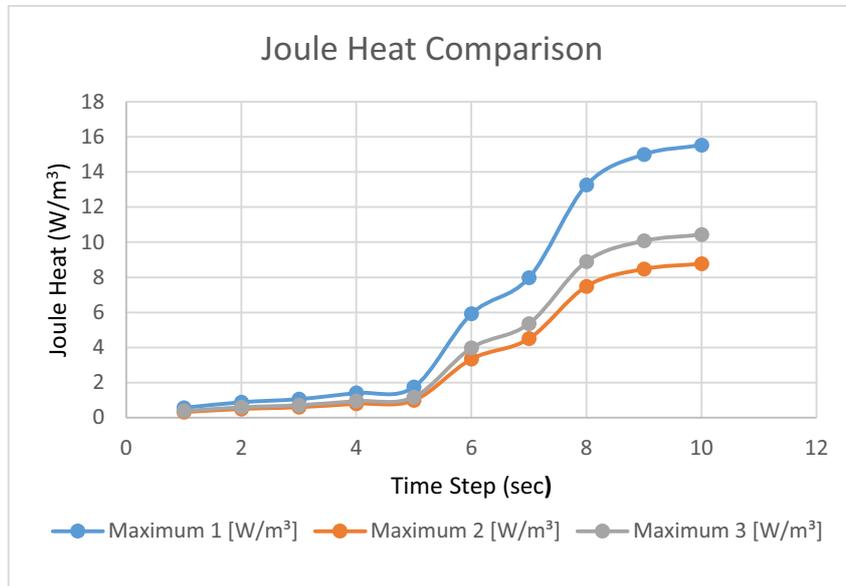
Figure 6(a). Joule heat comparison (525 V)

The Figure 6(a) provides the graphical representation of Joule Heat variation for 525 V. It is deduced that up to the 5th time step the values are almost similar but after this, the curve for Cast Iron rises almost exponentially when compared to the other materials. This is shown as the error percentage is between 2% and 7%.
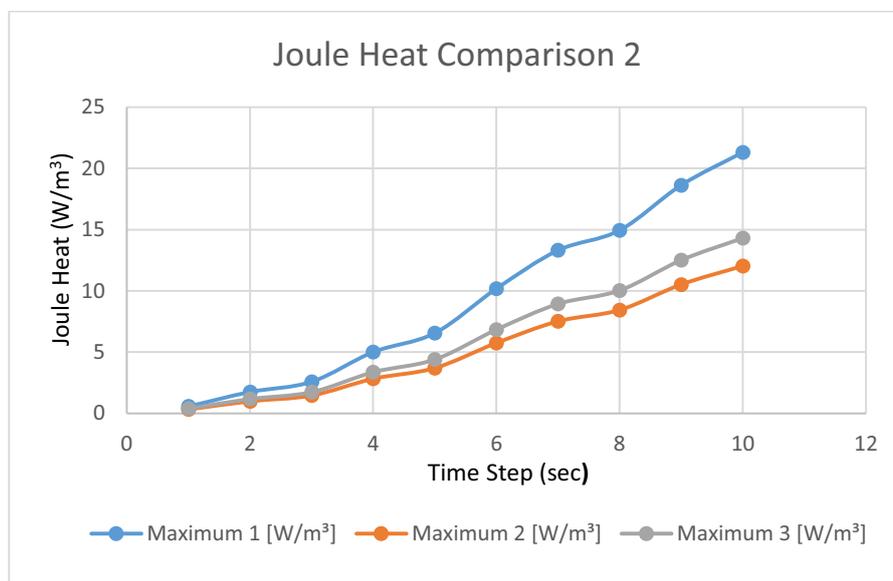
Figure 6(b). Joule Heat Comparison (615 V)

To test if this variation was constant, the input voltage was raised 615 V from the standard 525 V as shown in Figure 6(b). As expected, the values of Joule Heat for Cast Iron showed a similar rise after the

4th time step while the values for the other materials remained constant with a small error percentage throughout the range of the time steps. This led to the conclusion that based purely on the results of this analysis, Structural Steel might be used as a substitute for EN8C.
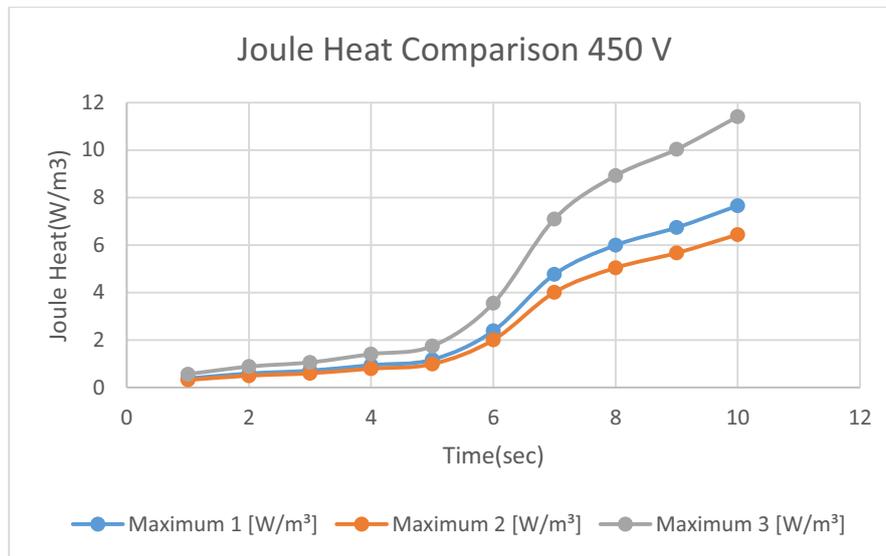
Figure 6(c). Joule Heat Comparison (450V)

From the graph in Figure 6(c), we can determine that as the input voltage is lowered, the values of Cast Iron and Structural Steel obtain a similar pattern of results while those of EN8C show a considerable difference of almost around 2-4 W/m^3. This voltage however does not provide a suitable threshold for the molecular structure to change to a martensitic structure and moreover shows us that the substitute materials used do not follow the same trends as the base material. From Figure 7(a) given above, we can determine that the rate of temperature drop is slightly more for Structural Steel = Cast Iron > EN8C. Upon comparison of the rate of change of heat fluxin Figure 7(b), it was found out that all the materials displayed a rise in the values of heat flux until the first-time step before falling steeply. Here also, the values for Cast Iron and Structural Steel were almost constant but the least heat flux drop was in EN8C.
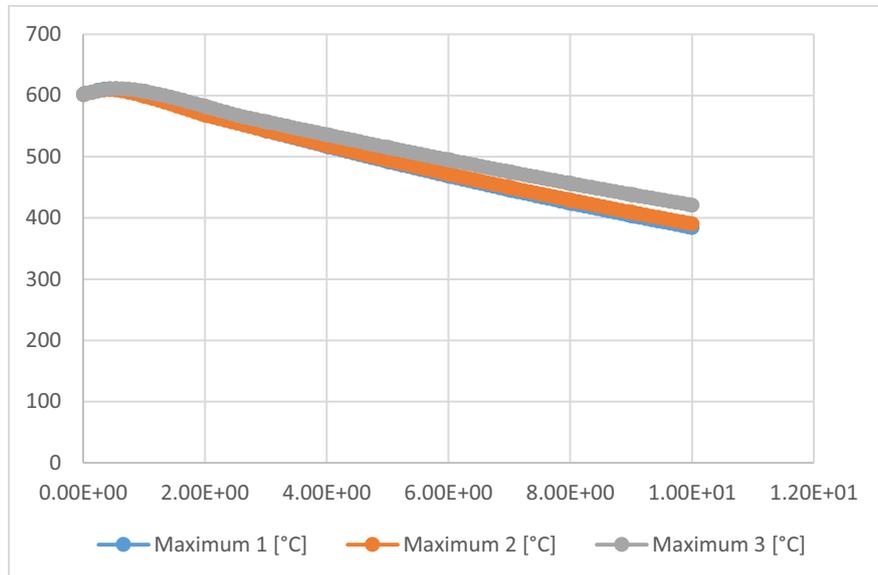
Figure 7(a). Temperature drop comparison
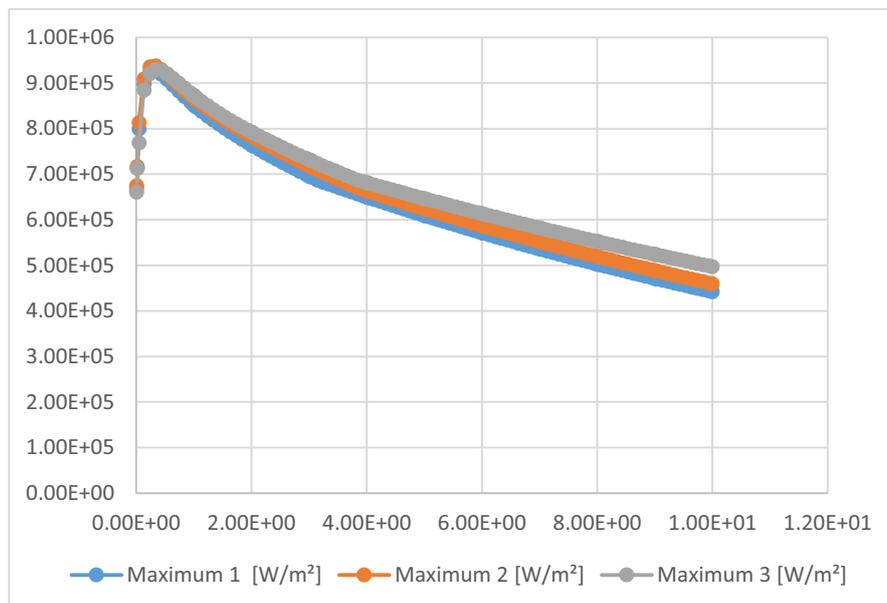
Figure 7(b). Heat flux variation comparison

With slight variations to the voltage and electric field, the output values can be different for the materials. To further observe the changes in this process, the variables constituting the non-linear analysis pattern in the analysis section must be changed to include other analyses such as impedance analysis with an increasing accuracy of the finite element analysis itself. It was also found out that with a decrease in the input voltage, the case depth of the material decreased from the front (teeth) side and remained almost constant from the back side. This means that any change in the voltage should be undertaken only upon

the specifications for the surface hardness and case depth being explicitly mentioned and tested after the process is completed. This matches with the inference made by Castallenos [11] "The overall efficiency of these systems is about 94% (near the resonance). The losses in the rectification stage can be assumed as 1% of the total efficiency. While remaining 5% may be related to inverter stage. In extreme cases, losses can be associated with an additional 5%". Furlani [12] has also verified these claims "maximum temperature values achieved in some nodes along a radius of the specimen and their correlation with the corresponding experimental final structures. In spite of the high heating rate at the surface of the specimen, the very high temperatures reached (about 1250 °C) in this zone are able to completely transform the external layer in austenite. The subsequent cooling phase induces in the material a complete martensitic micro-structure At intermediate zones, the maximum temperatures reached are in 600-700 °C interval, so that the transformation from perlite to austenite is almost complete (as well as the consequent austenite to martensite transformation), while the ferritic phase cannot transform itself into austenite."

4.Conclusions
With increasing differences in the shape of the surface that has to be hardened due to the wide variety of gears used in the market today, a multiple frequency pattern of induction hardening would be considered more productive as the output time can be reduced thus pushing out more components per batch. This would mean the incorporation of more number of coils in the heating process with each coil being supplied a set voltage in a different frequency and used to heat a different section of the component. This would enable the different sections of the component to come out with different hardness values based on the demand of the customer. Also, due to the constraints of having properties similar to the standard material, only two alternative materials have been analyzed through this simulation. However, any other material with similar composition can be included in this analysis. To determine the viability of the substitute to the standard material, further testing has to be conducted and various other parameters have to be verified to put this substitute into large scale production.

   Some advances in IH process as mentioned by O. Lucia [13] such as "One of the issues for the future of IH is the load adaptive capabilities and some solutions have been proposed. An adaptive simmering control of the temperature for a domestic induction cooker is required. Parameters are updated online, depending on the estimates provided by a multiple-model reset observer (MMReO). This observer consists of a reinitialized reset observer and of multiple fixed identification models."

References

[1] V Rudnev, D Loveless, R Cook and M Black (2003), *Induction Hardening of Gears: A   Review*, Heat treatment of   materials, p 97-103.

[2]   Robert S Ruffini, Robert T Ruffini, Valentin S Nemkov, Robert C Goldstein (2001), *Computer Simulation of Induction Heating*, FLUX Magazine.

[3] V Rudnev, *Single Coil Dual Frequency Induction Hardening of Gears*, Inductoheat group, 2009.

[4] I Magnabosco, P Ferro, A Tiziani, F Bonollo, *Induction Heat Treatment of a ISO C45 Steel bar; Experimental and Numerical analysis*, 2006, DTG University of Padova.

[5] D Coupard, Thierry Palin-luc, P Bristiel, V Ji, C Dumas, *Residual Stresses in Surface Induction Hardening of Steels: Comparison between Experiment and Simulation*, (2015), University of Bordeaux.

[6] G Breen, *Fatigue in Machine Structures (Ground Vehicles),* King's College (2015)

[7] J Yuan, J Kang, Yiming Rong, Richard D Sisson Jr, *FEM Modelling of Induction Hardening Process in Steel*, Worcester Polytechnic Institute, 10-01-2003.

[8]   P M C L Pacheco, M A Savi, A F Camarao, *Analysis of Residual Stresses Generated by Progressive Induction Hardening of Steel Cylinders*, Journal of Strain Analysis, **36**. No.5.

[9]   Xu Donghui, Li Zhonghua and Luo Jingxie, *Expressions for Predicting the Residual Stress in Surface Induction Hardening of Steel Bars*, Xian Jiaotong University (1995).

[10] K Palaniradja, N Alagumurthi and V Soundararajan, *Hardness and Case Depth Analysis through Optimization Techniques in Surface Hardening Processes*, The Open Materials Science Journal, (2010).

[11] E L Castellanos-Leal, D A Miranda, A E Coy, J G Barrero, J A González and O P Vesga Rueda, *Induction Hardening and Treatment and Simulation for Grey Cast Iron used in Engine Cylinders*, IOP Conf. Series Journal of Physics 786, 2017.

[12] Edward P Furlani, I Magnabosco, *Induction Heat Treatment of Steel: A Computer Simulation*, IEEE Transactions in Magnetics (1991).